

# Unique properties of transition metal quinone complexes of the MQ<sub>3</sub> series

Cortlandt G. Pierpont \*

*Department of Chemistry and Biochemistry, University of Colorado, Boulder, CO 80309, USA*

Received 6 October 2000; accepted 8 January 2001

Dedicated to Professor A.B.P. Lever on the occasion of his 65th birthday

## Contents

Abstract . . . . .	416
1. Introduction . . . . .	416
2. Complexes of the Cr, Mo, W triad as illustrations of metal-dependent shifts in charge distribution . . . . .	417
2.1 Chromium . . . . .	417
2.2 Molybdenum and tungsten . . . . .	419
2.3 Observations on complexes of the MQ <sub>3</sub> series with Cr, Mo and W . . . . .	421
3. Complexes of Mn, Tc, and Re: valence tautomerism and high-oxidation state complexes of Tc(VI) and Re(VI). . . . .	421
3.1 Manganese . . . . .	421
3.2 Technetium and rhenium . . . . .	423
3.3 Observations on complexes of the MQ <sub>3</sub> series with Mn, Tc and Re . . . . .	424
4. Complexes of Fe, Ru and Os: strong Fe(III)–SQ magnetic exchange and fluxional behavior as an indication of charge distribution . . . . .	424
4.1 Iron . . . . .	424
4.2 Ruthenium and osmium . . . . .	425
4.3 Observations on complexes of the MQ <sub>3</sub> series with Fe, Ru and Os . . . . .	427
5. Complexes of Co, Rh and Ir: metal mediated SQ–SQ magnetic exchange and periodic trends in charge distribution . . . . .	428
5.1 Cobalt. . . . .	428
5.2 Rhodium and Iridium. . . . .	429
5.3 Observations on complexes of the MQ <sub>3</sub> series with Co, Rh and Ir. . . . .	430
6. One MQ <sub>3</sub> complex of Ni: structural and magnetic properties of Ni <sup>II</sup> (3,6-DBBQ)(3,6-DBSQ) <sub>2</sub> . . . . .	431

\* Fax: + 1-303-4920951.

*E-mail address:* pierpont@colorado.edu (C.G. Pierpont).

7. Conclusion . . . . .	432
Acknowledgements . . . . .	432
References . . . . .	433

---

## Abstract

Transition metal complexes of ligands derived from *o*-benzoquinones have been shown to exhibit unique versatility in their electronic, structural and magnetic properties. Examples of these properties are described for complexes of the MQ<sub>3</sub> series with ligands coordinated in the form of semiquinonate (SQ) radical anions, catecholate dianions (Cat), and unreduced benzoquinones (BQ). Electrochemical activity may occur at either the metal or ligand; SQ complexes exhibit temperature dependent magnetic properties resulting from M–SQ, SQ–SQ, and intermolecular exchange coupling; equilibria between M<sup>I</sup>(SQ)/M<sup>II</sup>(Cat) redox isomers has been observed to occur in solution and in the solid state; charge localization has resulted in the formation of complexes containing mixed-valence ligands; strong  $\pi$  donation from Cat oxygens has been found to stabilize metal ions in unusually high oxidation states. Examples of these properties from among compounds of the MQ<sub>3</sub> series are described. © 2001 Elsevier Science B.V. All rights reserved.

**Keywords:** Transition metal complexes; *o*-Benzoquinones; MQ<sub>3</sub> series

---

## 1. Introduction

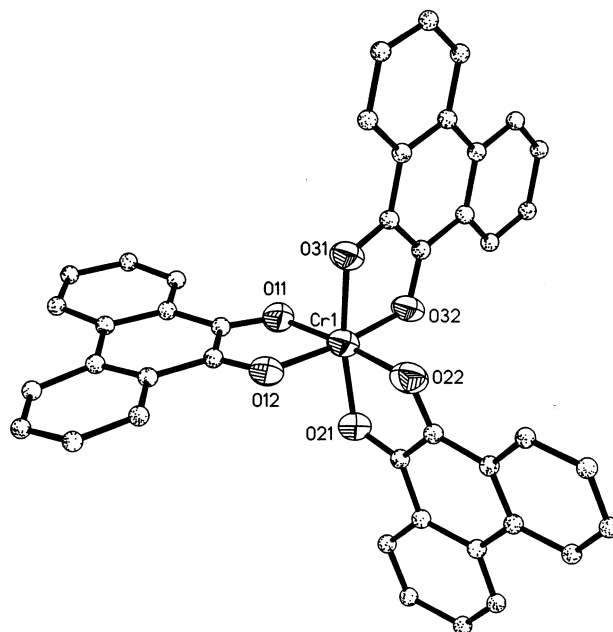
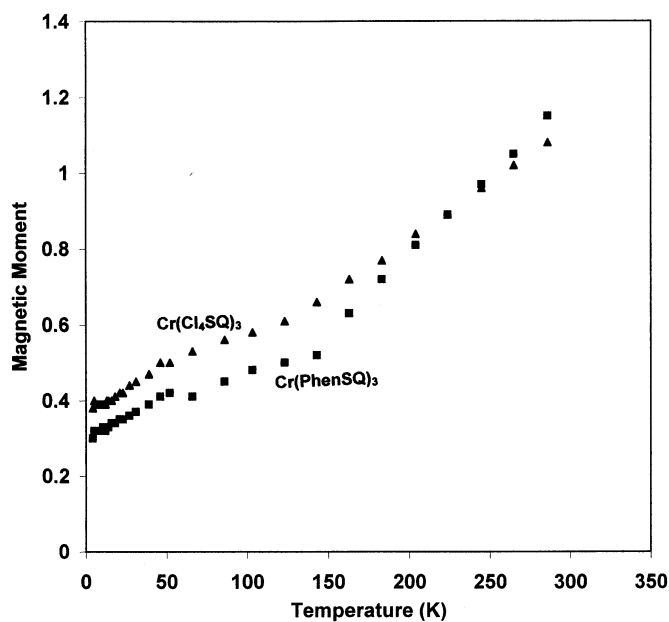
The focus in studies on coordination complexes is generally on the metal, and the electronic, magnetic, electrochemical, and structural properties that combine to give a unique chemical unit. Ligands associated with the metal as charge donors, or occasionally as  $\sigma$ -donor/ $\pi$ -acceptors, contribute to these properties through coordination. The oxidized 1,2-dithiolene/dithiolate complexes were found in the 1960s to exhibit unique properties that resulted from electronic metal–ligand charge delocalization as early exceptions to this view. In more recent work, diimine ligands (phen, bpy) and unsaturated macrocyclic polyimine ligands have been shown to have  $\pi$  orbitals accessible in low-energy MLCT processes and chemical reduction experiments. Nitrosyl ligands have been observed with linear, bent, and partially bent structures that are formally associated with the translocation of metal charge. Similar examples of redox isomerism exist for other ‘small molecule’ complexes, among them compounds containing peroxo/superoxo and dihydrogen/dihydride ligands. Over the past 25 years a wide variety of ligands have been found to contribute actively to the properties of complexes by modulating metal charge in compounds that have unique electronic properties resulting from metal–ligand charge delocalization or from isomerism associated with a formal transfer of charge between ligand and metal. As a distinction, redox isomerism requires that the properties of the metal ion conform in electronic and magnetic structure to a defined (or familiar) ionic state. Our focus in this review is on complexes of

transition metal ions that contain ligands derived from *o*-benzoquinones. Most commonly these ligands coordinate as semiquinonate radical anions (SQ) and catecholate dianions (Cat). Charge-localization presumes a defined charge for the metal ion, usually deduced from structural, magnetic and spectroscopic properties. Characterization on quinone complexes over the past 25 years has revealed ligand diversity that is without precedent in coordination chemistry. These features include observations on metal SQ–radical magnetic coupling [1], electron-transfer reactions between localized metal and ligand electronic levels that can be observed under equilibrium conditions in solid and solution [2], redox chemistry arising from either ligand or metal within an accessible potential range, and shifts in charge distribution associated with subtle changes in metal orbital energy. To focus the review further, we will restrict attention to complexes of the ‘MQ<sub>3</sub>’ series, where ligand charge, either BQ, SQ or Cat, is defined by the balance of M and Q frontier orbital energies.

## 2. Complexes of the Cr, Mo, W triad as illustrations of metal-dependent shifts in charge distribution

### 2.1. Chromium

Among the early examples of complexes containing multiple quinone ligands were the ‘M(Q)<sub>3</sub>’ complexes of Cr, Mo, and W [3]. They could be conveniently prepared by treating a neutral metal carbonyl complex, M(CO)<sub>6</sub>, with the parent benzoquinone. Crystallographic characterization on Cr<sup>III</sup>(Cl<sub>4</sub>SQ)<sub>3</sub>, prepared using tetrachloro-1,2-benzoquinone, showed that the complex was monomeric and octahedral [4]. Bond lengths to the metal and lengths within the quinone ligands are consistent with the Cr(III)–SQ formulation, although it was initially assumed that the electronic structure was delocalized like the 1,2-dithiolene analogs. Magnetic measurements on this complex and on the related complexes containing 9,10-phenanthrenesemiquinone (PhenSQ) (Fig. 1) revealed that they were paramagnetic at room temperature, in contrast with the diamagnetism of the dithiolene analogs, and that the magnetic properties were temperature-dependent [5]. The temperature dependence results from Cr(III)–SQ magnetic exchange that is intermediate in strength and dependent upon the quinone ligand. Magnetic moments for Cr<sup>III</sup>(Cl<sub>4</sub>SQ)<sub>3</sub> and Cr<sup>III</sup>(PhenSQ)<sub>3</sub> were near 1 μ<sub>B</sub> at room temperature and drop to values near zero at low temperature as is consistent with three *S* = 1/2 centers coupled antiferromagnetically with the *t*<sub>2g</sub> electrons of the *S* = 3/2 metal ion (Fig. 2). The related complex containing 3,5-di-*tert*-butyl-1,2-semiquinone appears diamagnetic at room temperature, but residual paramagnetism broadens the <sup>1</sup>H-NMR *tert*-butyl and ring proton resonances of the ligands. In surprising contrast, McCusker has found Cr<sup>III</sup>(3,6-DBSQ)<sub>3</sub> to be strongly paramagnetic at room temperature [6], pointing to a subtle, but significant, difference between 3,5- and 3,6-DBSQ.

Fig. 1. View of  $\text{Cr}^{\text{III}}(\text{PhenSQ})_3$ .Fig. 2. Temperature-dependent magnetic data for  $\text{Cr}^{\text{III}}(\text{Cl}_4\text{SQ})_3$  and  $\text{Cr}^{\text{III}}(\text{PhenSQ})_3$  plotted with data reported in Ref. [5].

The  $\text{Cr}^{\text{III}}(\text{SQ})_3$  complexes lie at the center of a ligand-based redox series since the  $\text{Cr}^{\text{III}}/\text{Cr}^{\text{II}}$  reduction potential lies outside the range of coordinated  $\text{SQ}/\text{Cat}$  reduction steps [7,8]. Structural features of  $[\text{Cr}^{\text{III}}(\text{Cat})_3]^{3-}$  support the reduced-quinone formulation, and recent characterization on members of the  $[\text{Cr}^{\text{III}}(\text{SQ})_2(\text{Cat})]^-$  series support the localized mixed-charge ligand formulation for intermediate members of the redox series [9]. EPR characterization on both  $[\text{Cr}^{\text{III}}(\text{SQ})_2(\text{Cat})]^-$  anions and  $[\text{Cr}^{\text{III}}(\text{SQ})_2(\text{BQ})]^+$  cations indicates that  $\text{Cr}^{\text{III}}-\text{SQ}$  magnetic coupling is strong, resulting in a metal-localized  $S = 1/2$  spin state in both cases [9,10]. Structural characterization and magnetic measurements performed by Kitagawa and coworkers on the  $[\text{Cr}(\text{X}_4\text{SQ})_2(\text{X}_4\text{Cat})]^-$  ( $\text{X} = \text{Cl}, \text{Br}$ ) anions, crystallized with cations that might promote lattice stacking interactions, agree with this observation [9]. Further, the anions were observed to show intense  $\text{Cat} \rightarrow \text{SQ}$  interligand intervalence transfer (LL/IT) transitions in the 2000–2500 nm region of the IR, a feature observed commonly for quinone complexes containing localized mixed-charge quinone ligands [2].

## 2.2. Molybdenum and tungsten

In contrast with the  $\text{Cr}^{\text{III}}(\text{SQ})_3$  charge distribution, the related complexes of Mo and W are  $\text{M}^{\text{VI}}(\text{Cat})_3$  species, although their structural features are sometimes more complicated than this formulation might suggest. Products obtained from the reaction of  $\text{Cl}_4\text{BQ}$  with  $\text{M}(\text{CO})_6$ ,  $\text{M} = \text{Mo}, \text{W}$ , are dimeric,  $[\text{M}_2(\text{Cl}_4\text{Cat})_6]$ , with two catecholate ligands that bridge adjacent metals (Fig. 3) [3,11]. Structural features of

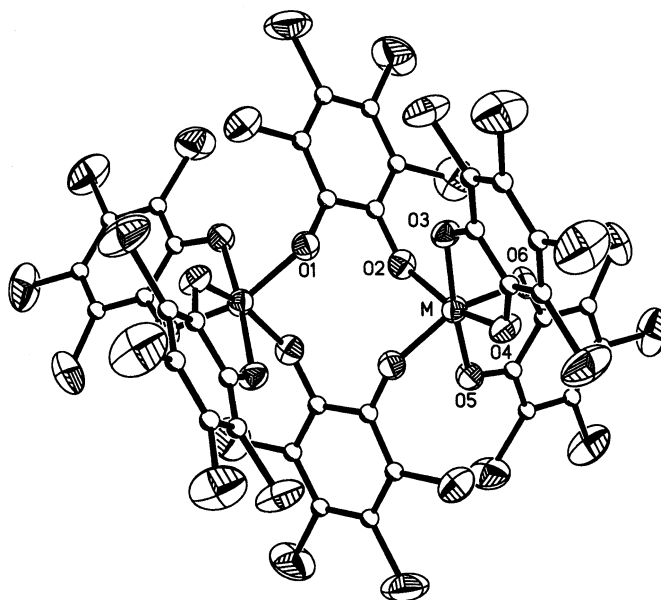


Fig. 3. View showing the bridging and chelating  $\text{Cl}_4\text{Cat}$  ligands of  $\text{M}_2(\text{Cl}_4\text{Cat})_6$ ,  $\text{M} = \text{Mo}, \text{W}$ .

the ligands agree with the catecholate charge, and electrochemical reduction steps occur at the metal. The related complex prepared with 9,10-phenanthrenequinone is best formulated as a mixed-charge ligand complex of Mo(V),  $\text{Mo}^{\text{V}}(\text{PhenSQ})\text{-(PhenCat)}_2$  [12]. The coordination geometry is trigonal prismatic, rather than octahedral, with adjacent complex molecules paired by charge transfer interactions between ligands of different charge. The Mo(V) charge formulation was not obvious in initial characterization on the complex, but subsequent information provided by detailed features of the ligands, together with weak residual paramagnetism arising from strong Mo(V)–SQ magnetic coupling, points to the  $\text{Mo}^{\text{V}}(\text{SQ})(\text{Cat})_2$  charge distribution.

Reactions carried out with  $\text{Mo}(\text{CO})_6$  and either 3,5-DBBQ or 3,6-DBBQ give initially an extremely oxygen-sensitive  $\text{Mo}(\text{DBQ})_3$  product [13,14]. With 3,5-DBBQ the product readily reacts with trace quantities of dioxygen to give the  $[\text{MoO}(\text{3,5-DBCat})_2]_2$  dimer [15]. Adjacent Mo(VI) centers are bridged by catecholate oxygen atoms at the exposed 1-ring position. *Tert*-butyl groups adjacent to both ring oxygens of 3,6-DBCat block bridging interactions. In this case, reaction with dioxygen appears to give the five-coordinate  $\text{Mo}^{\text{VI}}\text{O}(\text{3,6-DBCat})_2$  monomer in dilute solution. Upon concentration, oligomers form through oxo bridges. The chiral square tetramer  $[\text{Mo}(\mu\text{-O})(\text{3,6-DBCat})_2]_4$  has been isolated in crystalline form, Fig. 4 [14]. This difference between 3,5- and 3,6-DBBQ is important and appears in other aspects of MQ<sub>3</sub> coordination chemistry to be described below.

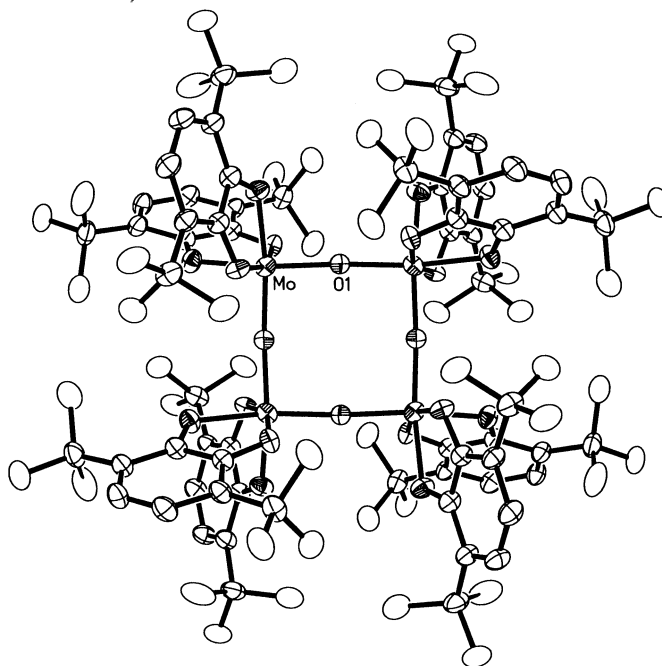


Fig. 4. The square  $\Delta\Delta\Delta\Delta$ - $[\text{MoO}(\text{3,6-DBCat})_2]_4$  tetramer obtained by condensation of  $\text{MoO}(\text{3,6-DBCat})_2$  units in toluene solution.

### 2.3. Observations on complexes of the $MQ_3$ series with Cr, Mo and W

- First row metals form complexes with partially-reduced SQ ligands. Second and third row metals form complexes of Cat ligands with high-oxidation state metals stabilized by strong  $\text{Cat} \rightarrow \text{M} \pi$ -donation.
- Complexes have localized charge distributions. Structural features of ligands are usually indicative of charge as BQ, SQ, or Cat. Occasionally, localized mixed-charge ligand complexes form that exhibit LL/IT transitions at low energy.
- Redox reactions are possible at either the metal or at the quinone ligands. This may lead to multiple redox steps for a single molecule and mixed-charge ligand products. The potential range of ligand-based redox series may be tuned using substituent bonding effects.
- Magnetic coupling between radical SQ ligands and  $d\pi$  ( $t_{2g}$ ) metal-localized spins can be strongly antiferromagnetic.

## 3. Complexes of Mn, Tc, and Re: valence tautomerism and high-oxidation state complexes of Tc(VI) and Re(VI)

### 3.1. Manganese

The synthetic approach of treating a metal carbonyl with an *o*-benzoquinone is an effective route to complexes of the SQ and Cat ligands. Reactions carried out with  $\text{Mn}_2(\text{CO})_{10}$  and either 3,5- or 3,6-DBBQ have been found to give products that reflect the structural difference of the *tert*-butyl substituents. With 3,5-DBBQ the Mn(II) tetramer,  $[\text{Mn}^{\text{II}}(3,5\text{-DBSQ})_2]_4$  is obtained, Fig. 5 [16]. Adjacent Mn centers are bridged by oxygens at the exposed 1-ring position of the SQ ligands. Magnetic properties show the effects of metal–SQ antiferromagnetic exchange. A related synthetic procedure carried out with 3,6-DBBQ gave a  $\text{Mn}(3,6\text{-DBQ})_3$  species [17]. Structural characterization has shown that it is monomeric and octahedral. Short Mn–O lengths, and intraligand bond lengths point to Mn(IV) in a formulation containing mixed-charge ligands, similar in charge distribution to Kitagawa's  $[\text{Cr}^{\text{III}}(\text{SQ})_2(\text{Cat})]^-$  anions [9]. The similarity extends further to the appearance of a low-energy Cat  $\rightarrow$  SQ LL/IT transition centered near 2300 nm for  $\text{Mn}^{\text{IV}}(3,6\text{-DBSQ})_2(3,6\text{-DBCat})$ . A charge distribution that is also possible is  $\text{Mn}^{\text{III}}(3,6\text{-DBSQ})_3$  that would differ structurally from  $\text{Mn}^{\text{IV}}(3,6\text{-DBSQ})_2(3,6\text{-DBCat})$  in having longer Mn–O lengths with the addition of an electron to the antibonding  $d\sigma$  ( $e_g$ ) orbital, and with the absence of the LL/IT band in the IR. Observations on the intensity of the LL/IT band with increasing temperature for a solid sample of  $\text{Mn}^{\text{IV}}(3,6\text{-DBSQ})_2(3,6\text{-DBCat})$  have been interpreted as indicating a shift in charge distribution to the Mn(III) redox isomer in a process that has been established for bis quinone complexes of Mn containing N-donor ligands, Fig. 6 [18].



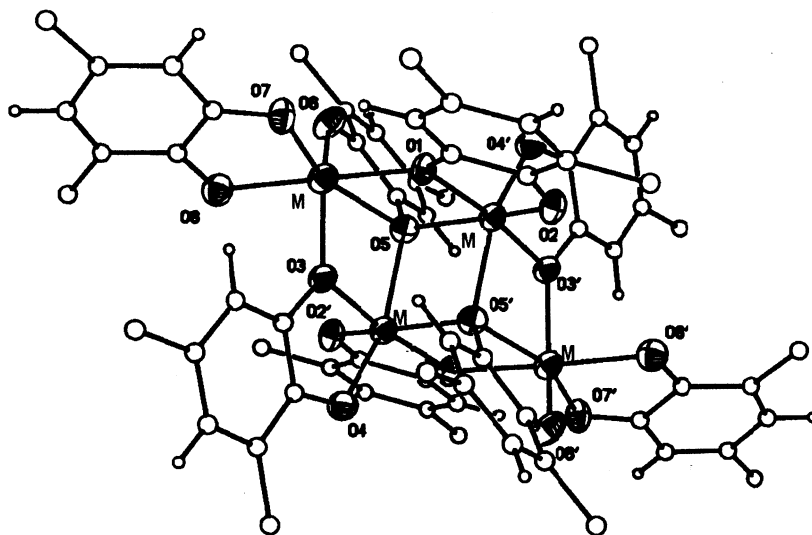


Fig. 5. View of the  $[M^{II}(3,5\text{-DBSQ})_2]_4$ ,  $M = \text{Mn, Co, Ni}$ , tetramer drawn with *t*-butyl methyl carbon atoms omitted.

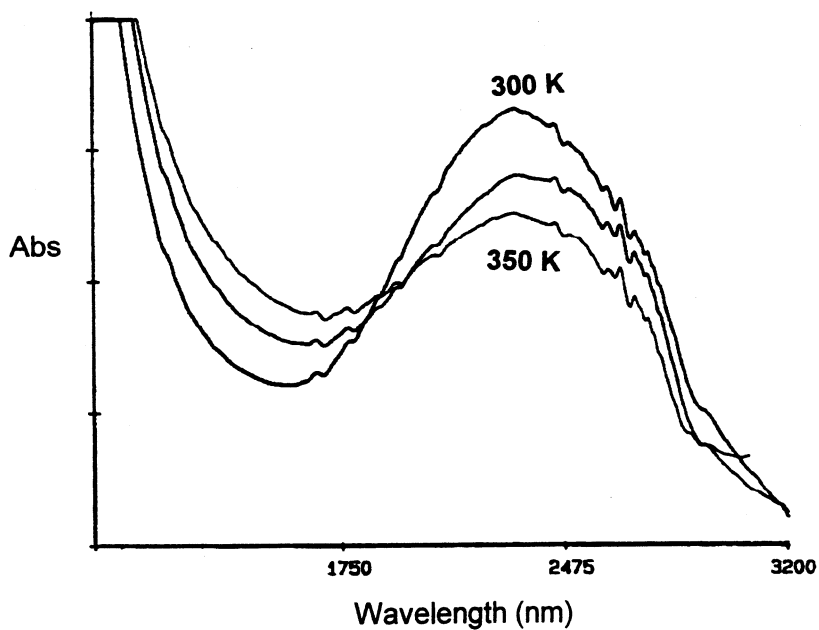


Fig. 6. Temperature-dependent changes in intensity of the Cat $\rightarrow$ SQ IT transition of  $\text{Mn}^{IV}(3,6\text{-DBSQ})_2(3,6\text{-DBCat})$  in the solid state with the shift to the  $\text{Mn}^{III}(3,6\text{-DBSQ})_3$  redox isomer.



A positive entropy change associated with the addition of charge to a ligand-directed  $d\sigma$  orbital, with the positive enthalpy change resulting, mainly, from changes in Mn–O bond strength, define the temperature range over which shifts in the Mn(IV)/Mn(III) equilibrium take place. In this case it happens to be somewhat above room temperature with a value for  $T_{1/2}$  near 350 K in solid and near 280 K in toluene solution.

### 3.2. Technetium and rhenium

Routes have been developed to the  $M^{VI}(\text{Cat})_3$  complexes of Tc and Re. Two procedures have been observed to give favorable results, either the  $M_2(\text{CO})_{10}/\text{BQ}$  approach described earlier for other metals, or reactions between the more accessible  $[\text{MO}_4]^-$  metal salts with the  $\text{H}_2\text{Cat}$  form of the quinone ligand [19,20]. These procedures have been used to form  $M^{VI}(\text{Cl}_4\text{Cat})_3$  and  $M^{VI}(3,5\text{-DBCat})_3$ ,  $M = \text{Tc}, \text{Re}$ , as unique complexes containing these metals in the hexavalent oxidation state without stabilizing terminal oxo ligands. The  $\text{Re}_2(\text{CO})_{10}$  route to  $d^1 \text{Re}^{VI}(\text{Cl}_4\text{Cat})_3$  proceeds through a stable  $\text{Re}^I(\text{CO})_4(\text{Cl}_4\text{SQ})$  intermediate containing a radical-based spin. Both complexes appear in EPR spectra obtained midway through the reaction, Fig. 7. Note the exceptionally strong hyperfine coupling to the  $I = 5/2$   $^{185,187}\text{Re}$  nuclei in Fig. 7 showing the metal-localized spin of the  $\text{Re}(\text{VI})$  center compared with the weakly coupled radical spectrum of the carbonyl complex.

Electrochemical characterization on the  $\text{Re}(\text{Cat})_3$  complexes shows a metal-based redox series consisting of an oxidation to  $[\text{Re}^{VII}(\text{Cat})_3]^+$ , and reductions to  $[\text{Re}^V(\text{Cat})_3]^-$  and  $[\text{Re}^{IV}(\text{Cat})_3]^{2-}$  [19,21]. Similarly,  $\text{Mn}^{IV}(3,6\text{-DBSQ})_2(3,6\text{-DBCat})$  undergoes two-step reduction to  $[\text{Mn}^{IV}(3,6\text{-DBCat})_3]^{2-}$  in reactions that are ligand-based.

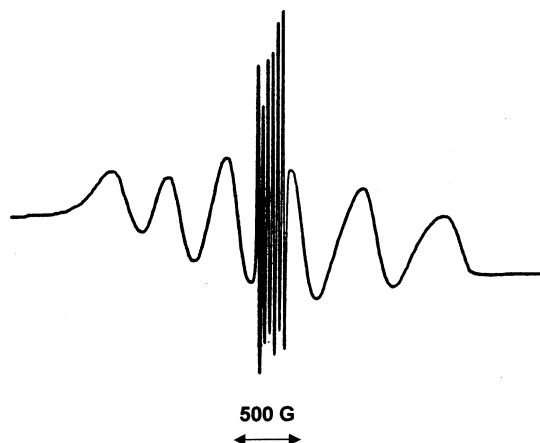


Fig. 7. EPR signal of  $\text{Re}(\text{Cl}_4\text{SQ})(\text{CO})_4$  (weak hyperfine) superimposed on the signal of  $\text{Re}^{VI}(\text{Cl}_4\text{Cat})_3$  during the reaction between  $\text{Re}_2(\text{CO})_{10}$  and  $\text{Cl}_4\text{BQ}$ .

### 3.3. Observations on complexes of the $MQ_3$ series with Mn, Tc and Re

- Valence tautomerism, as an equilibrium between redox isomers differing in charge distribution, is possible for charge-localized complexes of first row metals. Equilibrium conditions are defined by positive changes in entropy and enthalpy associated with charge transfer into antibonding metal orbitals directed at ligand coordination sites.
- Strong  $\pi$ -donation from filled oxygen orbitals of the Cat ligands stabilize second and third row metals in unusually high oxidation states. In this respect, Cat ligands are as effective as terminal oxo ligands.

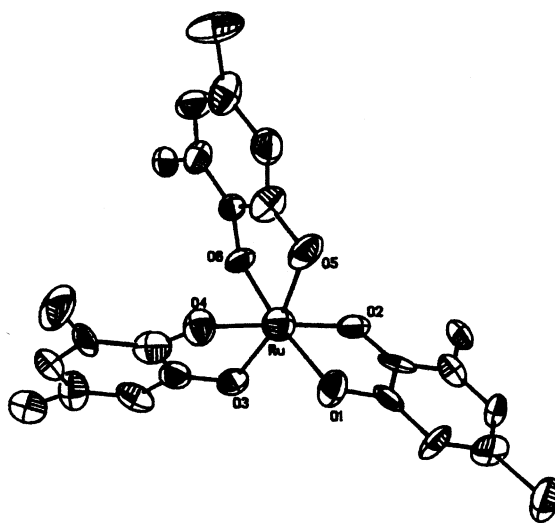
## 4. Complexes of Fe, Ru and Os: strong Fe(III)–SQ magnetic exchange and fluxional behavior as an indication of charge distribution

### 4.1. Iron

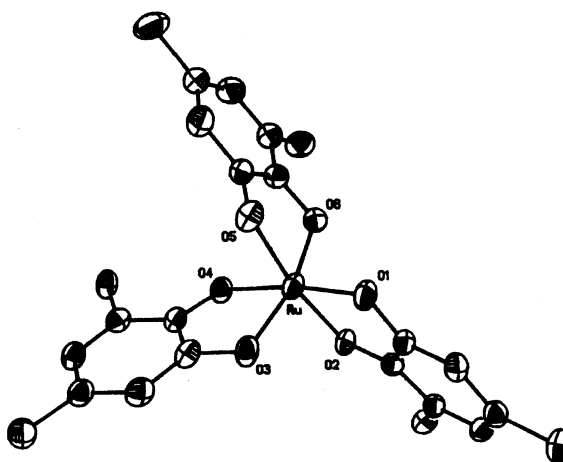
The  $Fe^{III}(SQ)_3$  series has been characterized in detail with the four common SQ ligands  $Cl_4SQ$ , PhenSQ, 3,5-DBSQ, and 3,6-DBSQ [22,23]. High-field Mössbauer spectra have established that the metal is  $hs-Fe(III)$  at all temperatures [24], and the magnetic properties of the complexes have been of interest in studies on metal–radical exchange. It is known from studies on octahedral complexes of  $Cr(III)$  and  $Ni(II)$  that SQ exchange with  $d\pi$  metal electrons is antiferromagnetic, while exchange with  $d\sigma$  spins can be strong and ferromagnetic [25]. The magnetic properties of  $Fe^{III}(3,5-DBSQ)_3$  support this view with a  $S = 1$  spin state at all temperatures resulting from strong  $d\pi$ –SQ magnetic exchange [22]. Related complexes of  $Cl_4SQ$  and PhenSQ show temperature dependence associated with thermal population of higher order spin states, and, at temperatures below 100 K, they have magnetic moments that drop well below the  $S = 1$  value. This is the result of intermolecular exchange, and crystallographic characterization on  $Fe(PhenSQ)_3$  has shown pairing interactions between ligands that appear commonly for complexes containing PhenSQ [22]. Magnetic measurements on  $Fe(3,6-DBSQ)_3$  show temperature-dependence not observed for  $Fe(3,5-DBSQ)_3$  [23], and weaker exchange that follows the pattern observed for the  $Cr(III)$  complexes of 3,5- and 3,6-DBSQ. An approximate fit was obtained for magnetic data measured above 50 K by using a Hamiltonian that contained contributions for both  $Fe$ –SQ and SQ–SQ exchange. Both interactions are antiferromagnetic, and  $J_{Fe-SQ}$  and  $J_{SQ-SQ}$  were strongly correlated in the model [23]. While meaningful quantitative values were not obtained, the best fit to experimental data was obtained for a value of  $J_{SQ-SQ}$  that was roughly twice the magnitude of  $J_{Fe-SQ}$ . Below 50 K experimental magnetic moment drops below the  $S = 1$  value, presumably due to an intermolecular component to exchange. Structural characterization on  $Fe(3,6-DBSQ)_3$  has shown that closest intermolecular contacts occur between ligand C–C bonds that have high concentrations of radical spin density, but separations are 4.0–4.5 Å.

#### 4.2. Ruthenium and osmium

The  $M(Q)_3$  complexes of Ru and Os have been prepared with 3,5-DBBQ [26]. There are no experimental features that point unambiguously to a specific charge distribution, however, short M–O lengths and relatively long C–O lengths for the quinone ligands point to a higher oxidation state for the metal than found for the  $Fe^{III}(SQ)_3$  series. Complexes of both metals are diamagnetic and both  $Ru(3,5-DBQ)_3$  and  $Os(3,5-DBQ)_3$  give sharp  $^1H$ -NMR spectra. Analysis of spectral differences for the two compounds provides some insight on charge distribution [27]. Unsymmetrical 3,5-DBQ gives two isomers for complexes of general form  $M(3,5-DBQ)_3$ , an isomer of  $C_3$  symmetry with *t*-butyl groups at the three-ring positions of the ligands all directed at a common triangular face of the octahedron, and an isomer of  $C_1$  symmetry with two *t*-butyl groups at one face and the third at the opposite face. As a final step in the synthesis of  $Ru(3,5-DBQ)_3$ , the two isomers were separated chromatographically to obtain crystalline samples of  $C_3$ - $Ru(3,5-DBQ)_3$  and  $C_1$ - $Ru(3,5-DBQ)_3$ , Fig. 8. Both isomers have been characterized crystallographically and they show characteristic  $^1H$ -NMR spectra consisting of six *t*-butyl and ring proton resonances for  $C_1$ - $Ru(3,5-DBQ)_3$  and two resonances each for  $C_3$ - $Ru(3,5-DBQ)_3$ . The octahedra are stereochemically rigid on an extended time scale. NMR spectra on  $Os(3,5-DBQ)_3$  recorded at room temperature consist of two resonances in the *t*-butyl region and two sharp resonances in the region of the ring protons. The spectrum resembles that of  $C_3$ - $Ru(3,5-DBQ)_3$ , but for spectra obtained on a sample that should contain both structural isomers. Spectra obtained at  $-85^\circ C$  ( $CD_2Cl_2$ ) show evidence for both isomers, however, with the  $C_1$  isomer present in highest concentration, Fig. 9. Resonances for the *t*-butyl protons are broadened at this temperature, but the temperature-dependent behavior of ring proton resonances indicate two temperature regimes. An increase in temperature from  $-85$  to  $-55^\circ C$  results in coalescence of two sets of two resonances for the  $C_1$  isomer, the third set of two resonances and the two resonances of the  $C_3$  isomer remain unchanged. A trigonal (or Bailar) twist results in exchange in environment of two ligands of the  $C_1$  isomer in a racemization process. Over a higher range in temperature, from  $-55$  to  $0^\circ C$ , resonances of the two sets of unique  $C_1$  ring protons coalesce, and coalesce with the proton resonances of the  $C_3$  isomer. This is the effect of a nondissociative isomerization process. Isomerization is viewed to involve a tetragonal twist mechanism that proceeds through an intermediate of different structure and of slightly higher activation energy (Ray–Dutt twist) [28]. Both processes involve changes that have trigonal prismatic intermediate structures. Ligand field effects contribute to an increase in TP activation energy for low-spin  $d$ -configurations greater than  $d^2$ . The fluxional character of  $Os(3,5-DBQ)_3$  and the rigidity of  $Ru(3,5-DBQ)_3$  appear to result from a difference in metal  $d$ -configuration and charge. From this property and the results of structure determinations that show generally shorter Os–O and longer ligand C–O bond lengths for the Os complex, we assign this as a complex of  $d^2$  Os(VI). As in the case of the catecholate complexes of Mo(VI), W(VI), Tc(VI), and Re(VI), this is an unusual oxidation state



**C<sub>1</sub>-Ru(3,5-DBQ)<sub>3</sub>**



**C<sub>3</sub>-Ru(3,5-DBQ)<sub>3</sub>**

Fig. 8. Structures of the stereochemically rigid C<sub>1</sub> and C<sub>3</sub> isomers of Ru(3,5-DBQ)<sub>3</sub>.

for the metal in the absence of terminal oxo ligands. The related complex of ruthenium appears to contain the metal in a charge that is intermediate between that of Fe<sup>III</sup>(3,5-DBSQ)<sub>3</sub> and Os<sup>VI</sup>(3,5-DBCat)<sub>3</sub>, showing a subtle periodic dependence in charge distribution for the Fe, Ru, Os triad of metals.

#### 4.3. Observations on complexes of the $MQ_3$ series with Fe, Ru and Os

- A satisfactory fit to the temperature-dependent magnetic properties of  $\text{Fe}(3,6\text{-DBSQ})_3$  has required consideration of intramolecular SQ–SQ coupling as well as Fe–SQ exchange.
- Periodic changes in d-orbital energy for the Fe, Ru, Os series, relative to the  $\pi$  orbital energy of the quinone ligand, result in a shift in charge distribution, from  $\text{Fe}^{\text{III}}(\text{SQ})_3$  to  $\text{Os}^{\text{VI}}(\text{Cat})_3$ , and with an intermediate charge distribution for the related complex of Ru.

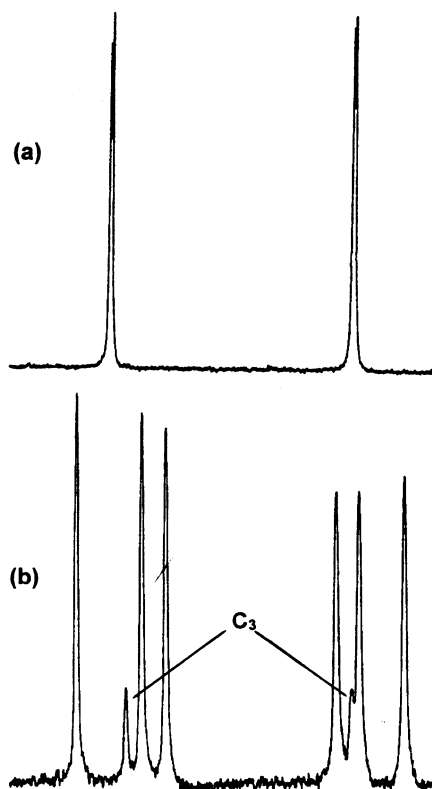


Fig. 9. Limiting  $^1\text{H}$ -NMR spectra on  $\text{Os}^{\text{VI}}(3,5\text{-DBCat})_3$  in the ring proton region recorded at (a)  $25^\circ\text{C}$  and (b)  $-85^\circ\text{C}$ .

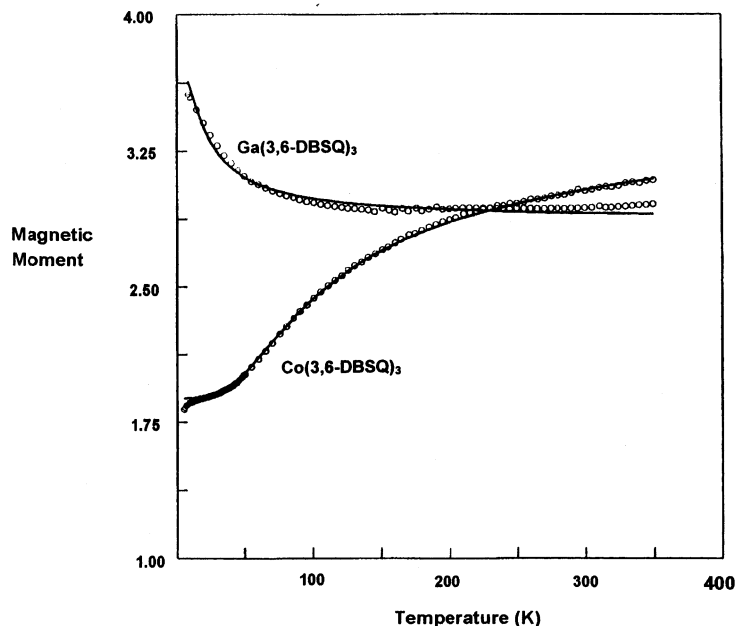


Fig. 10. Temperature-dependent changes in magnetic moment for  $\text{Co(3,6-DBSQ)}_3$  (antiferromagnetic) and  $\text{Ga(3,6-DBSQ)}_3$  (ferromagnetic).

## 5. Complexes of Co, Rh and Ir: metal mediated SQ–SQ magnetic exchange and periodic trends in charge distribution

### 5.1. Cobalt

The complexes of cobalt that have received greatest attention are of the  $\text{Co}^{\text{III}}(\text{N}-\text{N})(\text{SQ})(\text{Cat})/\text{Co}^{\text{II}}(\text{N}-\text{N})(\text{SQ})_2$  series in studies on valence tautomerism [2]. In the absence of a nitrogen donor ancillary ligand, the reaction between  $\text{Co}_2(\text{CO})_8$  and 3,5-DBBQ gives the  $[\text{Co}^{\text{II}}(3,5\text{-DBSQ})_2]_4$  tetramer [29], in a reaction that parallels the results obtained with Mn, Fe, and Ni, Fig. 5 [16,22]. The tetramer fails to undergo valence tautomerism, but it was of interest in early studies on magnetic exchange between radical ligands and paramagnetic transition metal ions [30]. A detailed analysis of magnetic properties is complicated by contributions from spin coupling interactions other than Co–SQ exchange and by the effects of zero-field splitting. As in the case of Mn, the reaction between  $\text{Co}_2(\text{CO})_8$  and 3,6-DBBQ gives a monomeric product due to the presence of *t*-butyl groups at ring positions adjacent to oxygens that bridge to adjacent metal ions in  $[\text{Co}^{\text{II}}(3,5\text{-DBSQ})_2]_4$ . The product of this reaction is  $\text{Co}^{\text{III}}(3,6\text{-DBSQ})_3$ , and with the diamagnetic, low-spin Co(III) ion at the center there is no metal–SQ spin coupling [31]. However, the magnetic properties of  $\text{Fe}^{\text{III}}(3,6\text{-DBSQ})_3$  indicated that SQ–SQ spin coupling may be as strong as Fe–SQ exchange, and  $\text{Co}^{\text{III}}(3,6\text{-DBSQ})_3$  has offered the opportu-

nity for study of SQ–SQ exchange mediated through the diamagnetic metal ion. The Kambé equation was used to model coupling between the three equivalent radical SQ ligands with the result that exchange was found to be antiferromagnetic and moderately strong with  $J = -39.1 \text{ cm}^{-1}$ , Fig. 10<sup>1</sup>. This result was presented with similar studies on  $\text{Ga}^{\text{III}}(3,6\text{-DBSQ})_3$  and  $\text{Al}^{\text{III}}(3,6\text{-DBSQ})_3$  which were shown to exhibit ferromagnetic coupling with  $J$  values of  $+6.2$  and  $+8.6 \text{ cm}^{-1}$ , respectively. These results demonstrate the potential significance of interrational exchange in the analysis of magnetic data on complexes containing multiple SQ ligands. The difference in the nature of coupling interactions for the d-block and p-block metals suggests a dependence on the metal orbital propagating spin coupling [32]. Recently, Wieghardt found that SQ–SQ coupling in a tris(iminosemiquinone)cobalt(III) complex is ferromagnetic, pointing to the significance of SQ orbital alignment, and reinforcing the importance of interrational exchange in multiradical complexes [33].

### 5.2. Rhodium and Iridium

Studies on complexes of the  $\text{MQ}_3$  series for Rh and Ir are incomplete. Dodsworth and Lever have described the electronic spectrum of  $\text{Rh}(3,6\text{-DBSQ})_3$  as consisting of transitions at 493 nm ( $6.2 \times 10^3 \text{ M}^{-1} \text{ cm}^{-1}$ ) and 935 nm ( $6.5 \times 10^3$ ), but without further description of the complex [34]. We have been able to isolate small quantities of dark blue  $\text{Ir}(3,6\text{-DBQ})_3$  as a minor product of the reaction between  $\text{Ti}(3,6\text{-DBSQ})$  and  $\text{K}_{0.6}[\text{Ir}(\text{CO})_2\text{Cl}_2] \cdot 0.5\text{H}_2\text{O}$  [35]. The electronic spectrum of  $\text{Ir}(3,6\text{-DBQ})_3$  consists of intense bands at 988 nm ( $14 \times 10^3$ ) and 641 nm ( $7 \times 10^3$ ) with a shoulder on the high energy side of the 641 band and bands of weaker intensity at 438 nm ( $2.4 \times 10^3$ ) and 1613 (630). Crystals of the complex form in a triclinic unit cell that is isomorphous with  $\text{Mn}(3,6\text{-DBSQ})_2(3,6\text{-DBCat})$ , and different from the higher symmetry monoclinic and orthorhombic cells of the  $\text{M}(3,6\text{-DBSQ})_3$ ,  $\text{M} = \text{Fe}, \text{Co}, \text{Ga}$ , series [23,31]. As in the case of  $\text{Mn}(3,6\text{-DBSQ})_2(3,6\text{-DBCat})$  detailed features of the structure suggest asymmetry in ligand charge with one appearing more clearly SQ in structure, while the other two are more catecholate in appearance, Fig. 11. EPR spectra recorded on powder samples at 77 K consist of a single broad resonance at  $g = 1.940$  and a half-field signal at  $g = 4.118$ . In toluene solution at room temperature there is no EPR signal. In a toluene glass at 77 K splitting appears on the  $g = 1.94$  signal from the effects of zero-field splitting and the half-field signal is present. These results point to a triplet spin state. However, ' $\text{Ir}(3,6\text{-DBQ})_3$ ' has an odd-electron configuration and it is reasonable that the complex has a  $S = 3/2$  spin ground state. The low-intensity signal in the  $g = 6$  region has gone unresolved [31]. These observations, with the absence of hyperfine splitting from the  $^{193,195}\text{Ir}$  isotopes, lead to a tentative formulation for the molecule under these conditions as  $\text{Ir}^{\text{III}}(3,6\text{-DBSQ})_3$ , similar to the complex of Co but in apparent contradiction with the crystallographic results. Unfortunately, the com-

<sup>1</sup> The Kambe equation for trimers exhibiting isotropic exchange was used to model experimental magnetic data for  $\text{Co}(3,6\text{-DBSQ})_3$  and  $\text{Ga}(3,6\text{-DBSQ})_3$ .  $H = -2J_{\text{SQ,SQ}}(S_1S_2 + S_1S_3 + S_2S_3)$ .

plex has not been obtained in sufficient quantity to permit magnetic measurements to unambiguously identify the spin ground state or to detect temperature-dependent shifts in charge distribution and magnetism.

### 5.3. Observations on complexes of the $MQ_3$ series with Co, Rh and Ir

- Metal-mediated SQ–SQ magnetic exchange contributes significantly to the magnetic properties of complexes containing multiple SQ ligands. The nature of the exchange interaction, ferromagnetic or antiferromagnetic, depends upon the symmetry of the metal orbitals linking the radical ligands and the symmetry of the ligand orbitals at the metal for unsymmetrical ligands.
- Observations on the  $MQ_3$  complexes of Rh and Ir are inconclusive. EPR spectra point to a  $Ir^{III}(3,6\text{-DBSQ})_3$  formulation, but structural features are more consistent with a  $Ir^V(3,6\text{-DBSQ})(3,6\text{-DBCat})_2$  charge distribution. The molecule appears not to have the  $M^{VI}(3,6\text{-DBCat})_3$  charge distribution of other third-row metals, and the inconsistency may arise from a shift in charge distribution similar to that observed for  $Mn(3,6\text{-DBSQ})_2(3,6\text{-DBCat})$ .

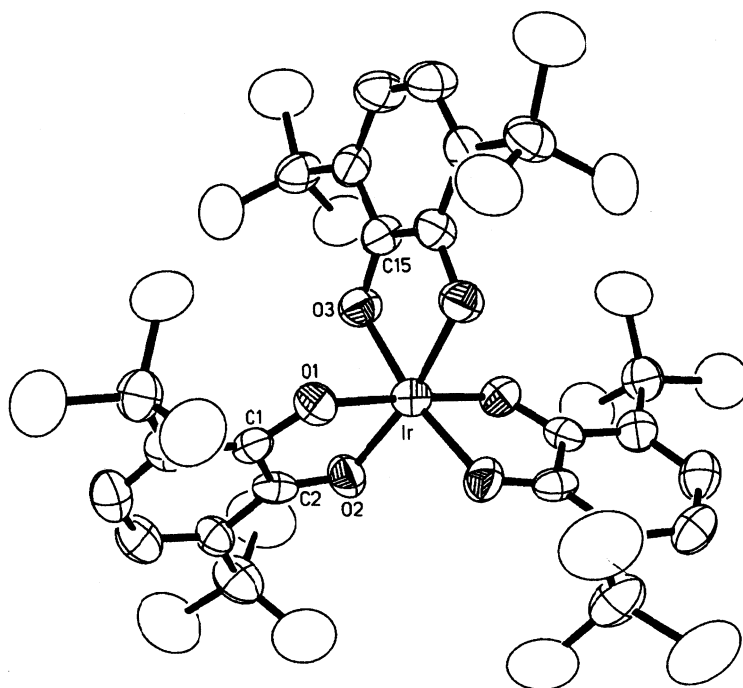


Fig. 11. View of  $Ir(3,6\text{-DBQ})_3$ . Bond lengths: Ir–O 1.957(8)–2.004(9) Å; C–O 1.298(14)–1.328(14) Å.



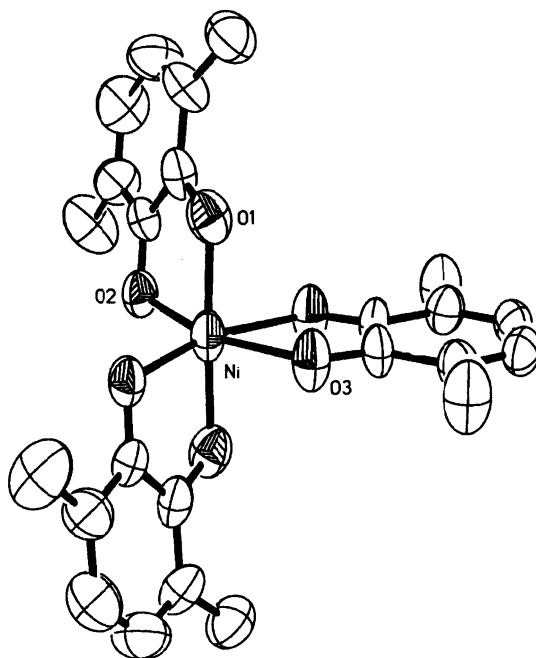


Fig. 12. View of  $\text{Ni}^{\text{II}}(3,6\text{-DBBQ})(3,6\text{-DBSQ})_2$ .

## 6. One $\text{MQ}_3$ complex of Ni: structural and magnetic properties of $\text{Ni}^{\text{II}}(3,6\text{-DBBQ})(3,6\text{-DBSQ})_2$

Quinone complexes of the Ni, Pd, Pt triad consist of  $\text{M}^{\text{II}}(\text{SQ})_2$  species formed by reactions between complexes of the zero-valent metals with 3,5-DBBQ. For palladium, the ‘ $\text{Pd}(3,5\text{-DBQ})$ ’ complex has been formed, but structural characterization has shown it to be  $\text{Pd}_2^0[\text{Pd}^{\text{II}}(3,5\text{-DBSQ})_2]_2$  [36]. Magnetic coupling between radical SQ ligands through the metals of square planar complexes is quite strong, leading to diamagnetism and sharp  $^1\text{H-NMR}$  resonances for the Pd and Pt complexes, and broadened resonances for the weakly paramagnetic Ni complex prepared with 3,6-DBBQ. The ‘ $\text{Ni}^{\text{II}}(3,5\text{-DBSQ})_2$ ’ analog of  $\text{Ni}^{\text{II}}(3,6\text{-DBSQ})_2$  is a tetramer with octahedral Ni(II) ions and a structure that is similar to the Co(II) and Mn(II) analogs (Fig. 5) [29]. Reactions used to form  $\text{Ni}^{\text{II}}(3,6\text{-DBSQ})_2$ , but carried out using excess benzoquinone, were found to form ‘ $\text{Ni}(3,6\text{-DBQ})_3$ ’ [37]. Structural characterization has indicated that the molecule contains quinone ligands of mixed charge coordinated to Ni(II) in  $\text{Ni}^{\text{II}}(3,6\text{-DBBQ})(3,6\text{-DBSQ})_2$ , Fig. 12. In contrast with the near diamagnetism of  $\text{Ni}^{\text{II}}(3,6\text{-DBSQ})_2$ ,  $\text{Ni}^{\text{II}}(3,6\text{-DBBQ})(3,6\text{-DBSQ})_2$  is strongly paramagnetic with a magnetic moment of  $4.57\mu_{\text{B}}$  that remains nearly constant to 20 K. This value is close to the moment that might result in the case of no interaction between the  $S = 1$  Ni(II) center and the two radical ligands ( $S = 1 + 2(S = 1/2)$ ). Prior magnetic characterization on octahedral  $[\text{Ni}(\text{N}_4)(\text{SQ})]^+$  and  $\text{Ni}(\text{N-N})(\text{SQ})_2$

complexes has shown that Ni–SQ exchange is weakly ferromagnetic due to the orthogonality of metal  $d\sigma$  and ligand  $\pi$  spins [25b,30]. Characterization on  $\text{Co(3,6-DBSQ)}_3$  indicated that SQ–SQ coupling should be antiferromagnetic. A model with ferromagnetic Ni–SQ and antiferromagnetic SQ–SQ exchange interactions may fit the data, but meaningful quantitative values for coupling constants have not been obtained.

## 7. Conclusion

Reactions between metal carbonyl complexes and *o*-benzoquinones offer simple routes to many of the  $\text{MQ}_3$  complexes. Complexes of the Ti triad include  $[\text{Ti}(\text{Cat})_3]^{2-}$  and  $[\text{Hf}(\text{Cat})_4]^{4-}$ , and SQ and Cat complexes of vanadium have appeared, but there is not sufficient detailed characterization on members of the Ti and V groups to identify periodic shifts in properties [38]. Consequently, our review has begun with members of the Cr, Mo and W series. First row metals give complexes with  $\text{M}^{\text{III}}(\text{SQ})_3$  charge distributions for  $\text{M} = \text{Cr}$  and  $\text{Fe}$ . The magnetic properties of these compounds have been of interest in studies on metal–radical exchange, although, intramolecular SQ–SQ coupling and intermolecular interactions complicate interpretation in terms of simple M–SQ coupled models [25c]. The charge-localized nature of quinone complexes is demonstrated by the formation of complexes with mixed charge quinone ligands for Mn and Ni. Valence tautomerism has been observed for  $\text{Mn(3,6-DBSQ)}_2(3,6\text{-DBCat})$  with a shift in charge distribution to  $\text{Mn(3,6-DBSQ)}_3$  at higher temperatures in solution and in the solid state. Complexes prepared with second and third row metals give  $\text{MQ}_3$  products with high oxidation state metal ions stabilized by strong  $\pi$  donation from Cat oxygen atoms. Unusual examples of Tc(VI) and Re(VI) have been obtained, but the pattern of  $\text{M}^{\text{VI}}(\text{Cat})_3$  species disappears for late metals as *d*-orbital energies stabilize across the period. The complexes of Pd and Pt resemble Ni, and a similar pattern may exist for the Co, Rh, Ir triad. The *o*-quinone ligands are unique in their ability to form complexes with the varied and unusual properties encountered for members of the ‘ $\text{MQ}_3$ ’ series.

## Acknowledgements

It is a pleasure to recognize the contributions of the scientists who carried out this research: Drs Robert Buchanan, Hartley Downs, Marion Cass, Brian Fitzgerald, Lynn deLearie, Scott Larsen, Glenn Fox, Steven Boone, Cathy Simpson, Samareesh Bhattacharya, Christopher Lange, Anne Whalen, and Attia Attia. We thank Professor David Hendrickson for collaboration on magnetic and Mössbauer measurements that led to initial assignments of charge distribution for many of the SQ complexes, and the National Science Foundation for continued support of this research (currently through grant CHE 9985970).

## References

- [1] A. Dei, D. Gatteschi, *Inorg. Chim. Acta* 198–200 (1992) 813.
- [2] (a) D.A. Shultz, in: J.S. Miller, M. Drillon (Eds.), *Magnetoscience — from Molecules to Materials*, Wiley–VCH, in press. (b) C.G. Pierpont, *Coord. Chem. Rev. (ICCC34 Issue)*, in press.
- [3] (a) C.G. Pierpont, H.H. Downs, T.G. Rukavina, *J. Am. Chem. Soc.* 96 (1974) 5573. (b) C.G. Pierpont, H.H. Downs, *J. Am. Chem. Soc.* 97 (1975) 2123.
- [4] C.G. Pierpont, H.H. Downs, *J. Am. Chem. Soc.* 98 (1976) 4834.
- [5] (a) R.M. Buchanan, H.H. Downs, W.B. Shorthill, C.G. Pierpont, S.L. Kessel, D.N. Hendrickson, *J. Am. Chem. Soc.* 100 (1978) 4318. (b) R.M. Buchanan, S.L. Kessel, H.H. Downs, C.G. Pierpont, D.N. Hendrickson, *J. Am. Chem. Soc.* 100 (1978) 7894.
- [6] J.K. McCusker, Personal communication.
- [7] H.H. Downs, R.M. Buchanan, C.G. Pierpont, *Inorg. Chem.* 18 (1979) 1736.
- [8] S.R. Sofen, D.C. Ware, S.R. Cooper, K.N. Raymond, *Inorg. Chem.* 18 (1979) 234.
- [9] H.-C. Chang, T. Ishii, M. Kondo, S. Kitagawa, *J. Chem. Soc. Dalton Trans.* (1999) 2467.
- [10] R.M. Buchanan, J. Claffin, C.G. Pierpont, *Inorg. Chem.* 22 (1983) 2552.
- [11] L.A. deLearie, R.C. Haltiwanger, C.G. Pierpont, *Inorg. Chem.* 27 (1988) 3842.
- [12] C.G. Pierpont, R.M. Buchanan, *J. Am. Chem. Soc.* 97 (1975) 4912.
- [13] M.E. Cass, C.G. Pierpont, *Inorg. Chem.* 25 (1986) 122.
- [14] C.-M. Liu, E. Nordlander, J. Andrew, B. Noll, C.G. Pierpont, Submitted for publication.
- [15] R.M. Buchanan, C.G. Pierpont, *Inorg. Chem.* 18 (1979) 1616.
- [16] M.W. Lynch, D.N. Hendrickson, B.J. Fitzgerald, C.G. Pierpont, *J. Am. Chem. Soc.* 106 (1984) 2041.
- [17] A.S. Attia, C.G. Pierpont, *Inorg. Chem.* 37 (1998) 3051.
- [18] A.S. Attia, C.G. Pierpont, *Inorg. Chem.* 34 (1995) 1172.
- [19] (a) L.A. deLearie, C.G. Pierpont, *J. Am. Chem. Soc.* 108 (1986) 6393. (b) L.A. deLearie, R.C. Haltiwanger, C.G. Pierpont, *Inorg. Chem.* 26 (1987) 817.
- [20] L.A. deLearie, R.C. Haltiwanger, C.G. Pierpont, *J. Am. Chem. Soc.* 111 (1989) 4324.
- [21] W.P. Griffith, C.A. Pumphrey, T.A. Rainey, *J. Chem. Soc. Dalton Trans.* (1986) 1125.
- [22] (a) R.M. Buchanan, S.L. Kessel, H.H. Downs, C.G. Pierpont, D.N. Hendrickson, *J. Am. Chem. Soc.* 100 (1978) 7894. (b) S.R. Boone, G.H. Purser, H.-R. Chang, M.D. Lowery, D.N. Hendrickson, C.G. Pierpont, *J. Am. Chem. Soc.* 111 (1989) 2292.
- [23] A.S. Attia, B.J. Conklin, C.W. Lange, C.G. Pierpont, *Inorg. Chem.* 35 (1996) 1033.
- [24] M.J. Cohn, C.-L. Xie, J.-P.M. Tuchagues, C.G. Pierpont, D.N. Hendrickson, *Inorg. Chem.* 31 (1992) 5028.
- [25] (a) D.E. Wheeler, J.K. McCusker, *Inorg. Chem.* 37 (1998) 2296. (b) C. Benelli, A. Dei, D. Gatteschi, L. Pardi, *Inorg. Chem.* 27 (1988) 2831. (c) C.G. Pierpont, A.S. Attia, *Collect. Czech. Chem. Commun.*, in press.
- [26] A.J. Nielson, W.P. Griffith, *J. Chem. Soc. Dalton Trans.* (1978) 1501.
- [27] S. Bhattacharya, S.R. Boone, G.A. Fox, C.G. Pierpont, *J. Am. Chem. Soc.* 112 (1990) 1088.
- [28] A. Rodger, B.F.G. Johnson, *Inorg. Chem.* 27 (1988) 3061.
- [29] R.M. Buchanan, C.G. Pierpont, *Inorg. Chem.* 18 (1979) 3439.
- [30] M.W. Lynch, R.M. Buchanan, C.G. Pierpont, D.N. Hendrickson, *Inorg. Chem.* 20 (1981) 1038.
- [31] C.W. Lange, B.J. Conklin, C.G. Pierpont, *Inorg. Chem.* 33 (1994) 1276.
- [32] (a) G.D. Perekhodtsev, Ya.S. Lebedev, *J. Struct. Chem.* 38 (1997) 41. (b) G.D. Perekhodtsev, Ya.S. Lebedev, *J. Struct. Chem.* 38 (1997) 884.
- [33] C.N. Verani, S. Gallert, E. Bill, T. Weyhermüller, K. Wieghardt, P. Chaudhuri, *Chem. Commun.* (1999) 1747.
- [34] E.S. Dodsworth, A.B.P. Lever, *Chem. Phys. Lett.* 172 (1990) 151.
- [35] C.W. Lange, Thesis, University of Colorado, 1994.
- [36] G.A. Fox, C.G. Pierpont, *Inorg. Chem.* 31 (1992) 3718.
- [37] C.W. Lange, C.G. Pierpont, *Inorg. Chim. Acta* 263 (1997) 219.
- [38] C.G. Pierpont, C.W. Lange, *Prog. Inorg. Chem.* 41 (1994) 331.